



THE UNIVERSITY *of* EDINBURGH

## Edinburgh Research Explorer

# Water vapour transport associated with tropical-temperate trough systems over southern Africa and the southwest Indian Ocean

### Citation for published version:

Todd, MC, Washington, R & Palmer, PI 2004, 'Water vapour transport associated with tropical-temperate trough systems over southern Africa and the southwest Indian Ocean', *International Journal of Climatology*, vol. 24, no. 5, pp. 555-568. <https://doi.org/10.1002/joc.1023>

### Digital Object Identifier (DOI):

[10.1002/joc.1023](https://doi.org/10.1002/joc.1023)

### Link:

[Link to publication record in Edinburgh Research Explorer](#)

### Document Version:

Publisher's PDF, also known as Version of record

### Published In:

International Journal of Climatology

### Publisher Rights Statement:

Published in International Journal of Climatology by the Royal Meteorological Society (2004)

### General rights

Copyright for the publications made accessible via the Edinburgh Research Explorer is retained by the author(s) and / or other copyright owners and it is a condition of accessing these publications that users recognise and abide by the legal requirements associated with these rights.

### Take down policy

The University of Edinburgh has made every reasonable effort to ensure that Edinburgh Research Explorer content complies with UK legislation. If you believe that the public display of this file breaches copyright please contact [openaccess@ed.ac.uk](mailto:openaccess@ed.ac.uk) providing details, and we will remove access to the work immediately and investigate your claim.



## WATER VAPOUR TRANSPORT ASSOCIATED WITH TROPICAL–TEMPERATE TROUGH SYSTEMS OVER SOUTHERN AFRICA AND THE SOUTHWEST INDIAN OCEAN

MARTIN C. TODD<sup>a,\*</sup> RICHARD WASHINGTON<sup>b</sup> and PAUL I. PALMER<sup>c</sup>

<sup>a</sup> *Department of Geography, University College London (UCL), 26 Bedford Way, London WC1H 0AP, UK*

<sup>b</sup> *School of Geography and the Environment, University of Oxford, Oxford OX1 3TB, UK*

<sup>c</sup> *Earth and Planetary Sciences, Harvard University, 29 Oxford Street, Cambridge, MA 02138, USA*

*Received 13 February 2002*

*Revised 11 January 2004*

*Accepted 17 January 2004*

### ABSTRACT

Tropical–temperate trough (TTT) systems are the dominant rain-producing synoptic type over southern Africa. They represent an important mechanism of poleward transport of energy and momentum. This paper provides an analysis of water vapour transport in TTT systems. An objective sampling of TTT systems is conducted from analysis of daily satellite rainfall products. During the sampled TTT events, rain bands extend from tropical southern Africa near 10°S to the midlatitudes of the southwest Indian Ocean. The divergent and non-divergent (streamfunction) components of vertically integrated water vapour flux associated with major TTT events are calculated, from National Centers for Environmental Prediction reanalysis data. During TTT events the streamfunction circulation dominates water vapour transport, although adjustments to the divergent component are relatively more important. The results indicate that TTT events facilitate a substantial water vapour flux from the tropics into the midlatitudes. Water vapour transport to the midlatitudes along the TTT axis is facilitated largely by changes to the streamfunction, associated with a strengthening and eastward displacement of the Indian Ocean high, and the advent of midlatitude transients. It is also shown that TTT systems are major regions of moisture convergence. The high vapour concentrations along the full extent of the TTT rain bands are maintained by the divergent circulation. The structure of these divergent vapour flux anomalies is suggestive of adjustments to the Walker circulation, involving strong anomalous divergence over the maritime continent/west Pacific and a weaker enhancement of the major divergence centre over the tropical Atlantic. Copyright © 2004 Royal Meteorological Society.

KEY WORDS: water vapour transport; divergent flow; non-divergent flow; tropical–temperate; southern Africa; southwest Indian Ocean

### 1. INTRODUCTION

Rainfall variability over southern Africa (SA) has long been the subject of investigation, due in part to the importance of rain-fed agriculture in the region, the arid to semi-arid nature of the climate, and the high degree of interannual and interdecadal variability observed over the region. The nature of such rainfall variability over SA has been investigated on numerous time scales, including the synoptic (Harrison, 1984, 1986; Diab *et al.*, 1991; Nasser and Jury, 1997; Parker and Jury, 1999), though interannual (Janowiak, 1988; Jury, 1992, 1997; Jury *et al.*, 1992; Nicholson and Kim, 1997; Rocha and Simmonds, 1997; Goddard and Graham, 1999; Landman and Mason, 1999; Cook, 2000, 2001; Nicholson and Selato, 2000; Nicholson *et al.*, 2001) to decadal and millennial time scales (Tyson, 1986; Cohen and Tyson, 1995; Stokes *et al.*, 1997; Folland *et al.*, 1998). For a review of variability on all these time scales see Mason and Jury (1997).

It is known that a dominant proportion of austral summer (wet season) rainfall over much of SA is derived from synoptic-scale tropical–temperate trough (TTT) systems that extend over both continental SA and the

\*Correspondence to: Martin C. Todd, Department of Geography, University College London (UCL), 26 Bedford Way, London WC1H 0AP, UK; e-mail: m.todd@geog.ucl.ac.uk

adjacent southwest Indian Ocean (SWIO; Harrison, 1984, 1986; Todd and Washington, 1998; Washington and Todd, 1999). During TTT events a band of cloud and rain links tropical convection over Africa with transients in the midlatitudes. SA and the SWIO is one of three known preferred locations for such tropical–temperate interaction in the Southern Hemisphere (Streten, 1973). Unlike its counterparts, namely the South Atlantic and South Pacific convergence zones (SACZ and SPCZ respectively), the SA–SWIO feature, referred to as the south Indian convergence zone (SICZ; Cook, 2000), is not semi-permanent and exists only during the austral summer months.

Peak summer rainfall in the SA–SWIO region is associated with the ITCZ, located over central SA at about 10°S extending eastward over the Indian Ocean (Figure 1). A diagonal band of high rainfall extends from central Africa southeastward to the midlatitudes over the SWIO at about 60°E, representing the SICZ (Figure 1). Studies of the structure of TTT cloud bands (Harrison, 1984, 1986, Todd and Washington, 1998; Washington and Todd, 1999) suggest that this mean rainfall structure reflects the location of these synoptic-scale systems. Variability in the location and frequency of occurrence of the SA–SWIO TTT cloud band has important implications for rainfall in the region.

Synoptic-scale major TTT events over SA–SWIO result from large-scale planetary circulation patterns. Adjustments to this circulation have considered the planetary wave structure, with variability in wave 5 dominant (Todd and Washington, 1999a). Large-scale water vapour transport anomalies may also be expected to occur in association with TTTs. Convergent fluxes form a pronounced poleward flux along the cloud band, suggesting that TTT events act as a major mechanism of poleward transfer of moisture (D’Abreton and Lindesay, 1993; Todd and Washington, 1999a). The significance of TTTs over SA and SWIO in the transfer of energy and momentum between tropical and temperate latitudes has been analysed by Harrison (1984, 1986) and Palmer *et al.* (2004).

There is evidence that the source regions for the poleward flux of water vapour lie well outside the local region (D’Abreton and Tyson, 1995; Todd and Washington, 1999a). Although the regional water vapour flux patterns associated with interannual rainfall anomalies over continental SA at the monthly scale have been comprehensively described (D’Abreton and Lindesay, 1993; D’Abreton and Tyson, 1995), no study to date

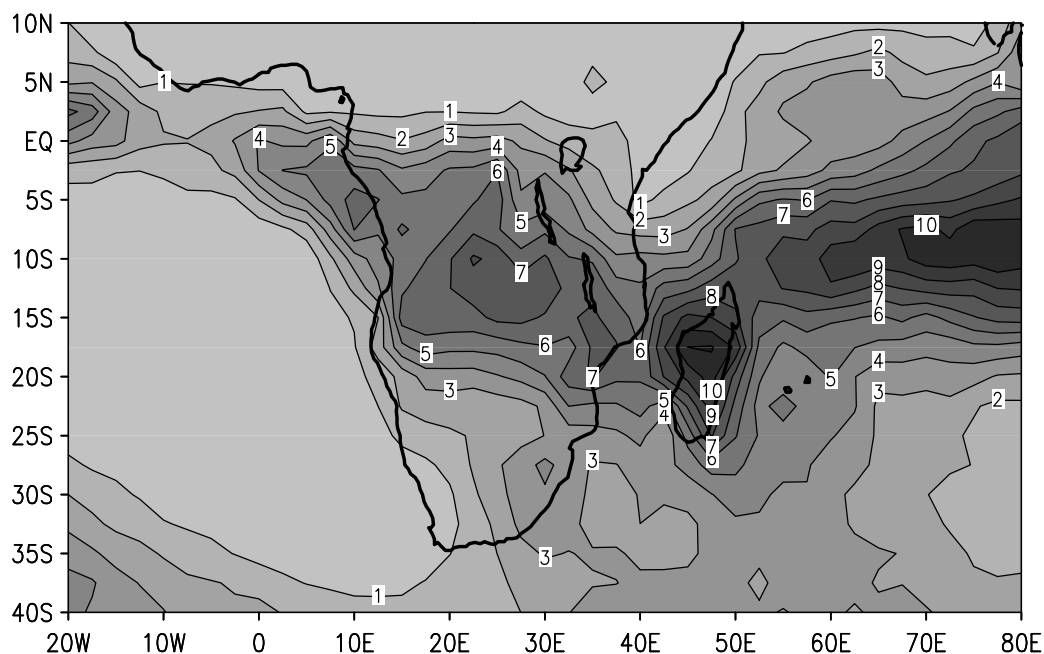


Figure 1. Mean summer (December–February) rainfall ( $\text{mm day}^{-1}$ ) as estimated by the Climate Prediction Center Merged Analysis of Precipitation (CMAP) rainfall product, derived from a combination of satellite infrared and passive microwave measurements, rain-gauge observations and numerical modelled fields (Xie and Arkin, 1997)

has objectively identified and quantified water vapour transport or the source and sink regions during TTT events over SA–SWIO. This paper addresses these question using the objective definition of TTT events of Todd and Washington (1998, 1999a; Washington and Todd, 1999) in combination with global reanalysis data.

## 2. DATA AND METHODOLOGY

Todd and Washington (1998; Washington and Todd, 1999) conducted empirical orthogonal function (EOF) analysis on 8 years of daily satellite rainfall for each of the austral summer months over the domain bounded by latitude 15–40°S and longitude 7.5–70°E. Rainfall was estimated using the reconstructed geostationary precipitation index (RGPI; Todd and Washington, 1999b). In the austral summer months of November–January the principal mode of daily rainfall variability is a dipole structure oriented northwest (NW) to southeast (SE) across SA and the SWIO (Figure 2). This loading pattern represents the preferred location of TTT features. In February, a single tropical–temperate rain band links central and southeast SA with the SWIO.

From the EOF time coefficients, the major extreme positive (negative) events typical of the leading EOF in each month were objectively identified by extracting days with time coefficients above (below) one standard deviation from the mean (Table I, Figure 3). These episodes represent the major events associated with the centres of activity of the TTT rainfall dipole structure. Positive events account for a larger portion of rainfall variance than do negative events over eastern SA and the SWIO, and they result in larger rainfall and circulation anomalies (Todd and Washington, 1998; Todd and Washington, 1999a). Therefore, in this paper we will consider only positive events in each month. During these TTT events, a cloud and rain band is positioned NW–SE extending from eastern SA to the midlatitudes of the SWIO.

These TTT events form the basis of composites for which the mean and mean anomalies of daily vertically integrated water vapour flux are calculated from averages of 12-hourly global analyses (on a 2.5° grid) from the National Center for Environmental Prediction (NCEP) reanalysis project (Kalnay *et al.*, 1996). In this study, data from the 1000 hPa–300 hPa levels were used and hereafter all references to vapour flux refer to the vertically integrated quantity. The significance of composite anomalies was tested using a *t*-test.

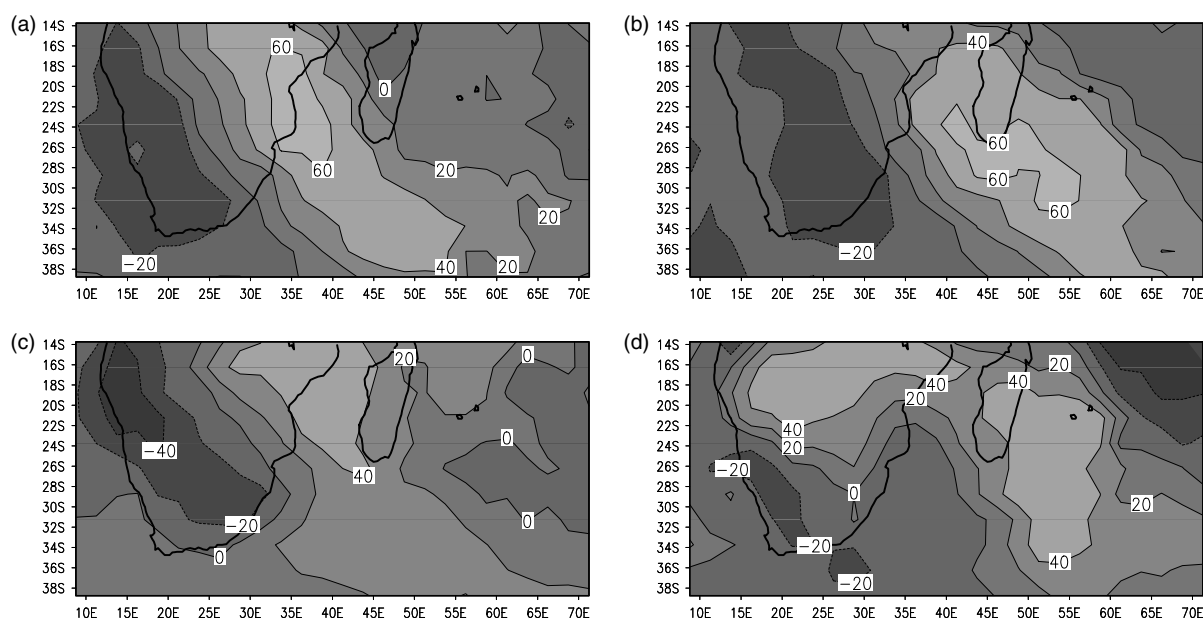


Figure 2. Leading EOF (derived from daily RGPI estimates of rainfall over the period 1986–93) loading pattern for (a) November, (b) December, (c) January and (d) February (adapted from Washington and Todd (1999))

Table I. Dates of daily data used to form composites of positive TTT events

Year	November	December	January	February
1986	9, 28	9–14, 22, 23, 30, 31	1, 5–9	6–10
1987	—	—	1–5, 23–26	—
1989	4, 10, 16, 27–30	3, 18–20	—	—
1990	24, 25	—	1–3	7, 11
1991	14–16, 20–22	5	10, 11	10, 14–17
1992	17, 25	24–27	—	—
1993	—	—	11–20	2, 8, 11–16, 22–25

The vertically integrated vector water vapour flux is defined as

$$\mathbf{Q} = \frac{1}{g} \int_{p_u}^{p_L} q \mathbf{v} dp \quad (1)$$

where the total wind vector  $\mathbf{v}$  is composed of the zonal and meridional components,  $q$  is specific humidity,  $g$  is the acceleration due to gravity,  $p_L$  and  $p_U$  are 1000 hPa and 300 hPa respectively. This vector water vapour flux can be considered to be composed of scalar rotational and irrotational (divergent) components

$$\mathbf{Q} = \mathbf{Q}_\psi + \mathbf{Q}_\chi \quad (2)$$

where the subscripts  $\psi$  and  $\chi$  denote the rotational and divergent components respectively. The Helmholtz relation (Equation (3)) describes how a vector may be decomposed into its components

$$\mathbf{Q} = \hat{\mathbf{k}} \times \nabla \psi - \nabla \chi \quad (3)$$

where  $\hat{\mathbf{k}}$  represents the vertical unit direction vector, and  $\chi$  and  $\nabla$  represent the vector curl and del operators respectively. The  $\psi$  and  $\chi$  fields of  $\mathbf{Q}$  can be obtained from Equation (3) through the application of curl and divergence operators respectively:

$$\nabla^2 \psi = \hat{\mathbf{k}} \cdot \nabla \times \mathbf{Q} \quad (4)$$

$$-\nabla^2 \chi = \nabla \cdot \mathbf{Q} \quad (5)$$

Solution of Equations (4) and (5) is found using spectral methods, which eliminates the computational problems than can be induced by polar singularities (Adams and Swarztrauber, 1997).

The resulting scalar fields are commonly known as the streamfunction  $\psi$  and velocity potential  $\chi$  fields. In the Southern Hemisphere, vapour transport is defined as cyclonic (anticyclonic) around streamfunction maxima (minima). Positive (negative) velocity potential values indicate water vapour divergence (convergence) and this transport occurs perpendicular to  $\chi$  contours and is proportional to the local  $\chi$  gradient. Water vapour divergence can be related to the water budget through

$$\nabla^2 \chi = P - E \quad (6)$$

where  $E$  is evaporation and  $P$  is precipitation. Over extended periods (such as the composite periods defined for this study)  $\chi$  is, therefore, an indicator of water vapour sources ( $E > P$ ) and sinks ( $P > E$ ) and effectively balances the deficit between local evaporation and precipitation (Chen, 1985; Piexoto and Oort, 1991).

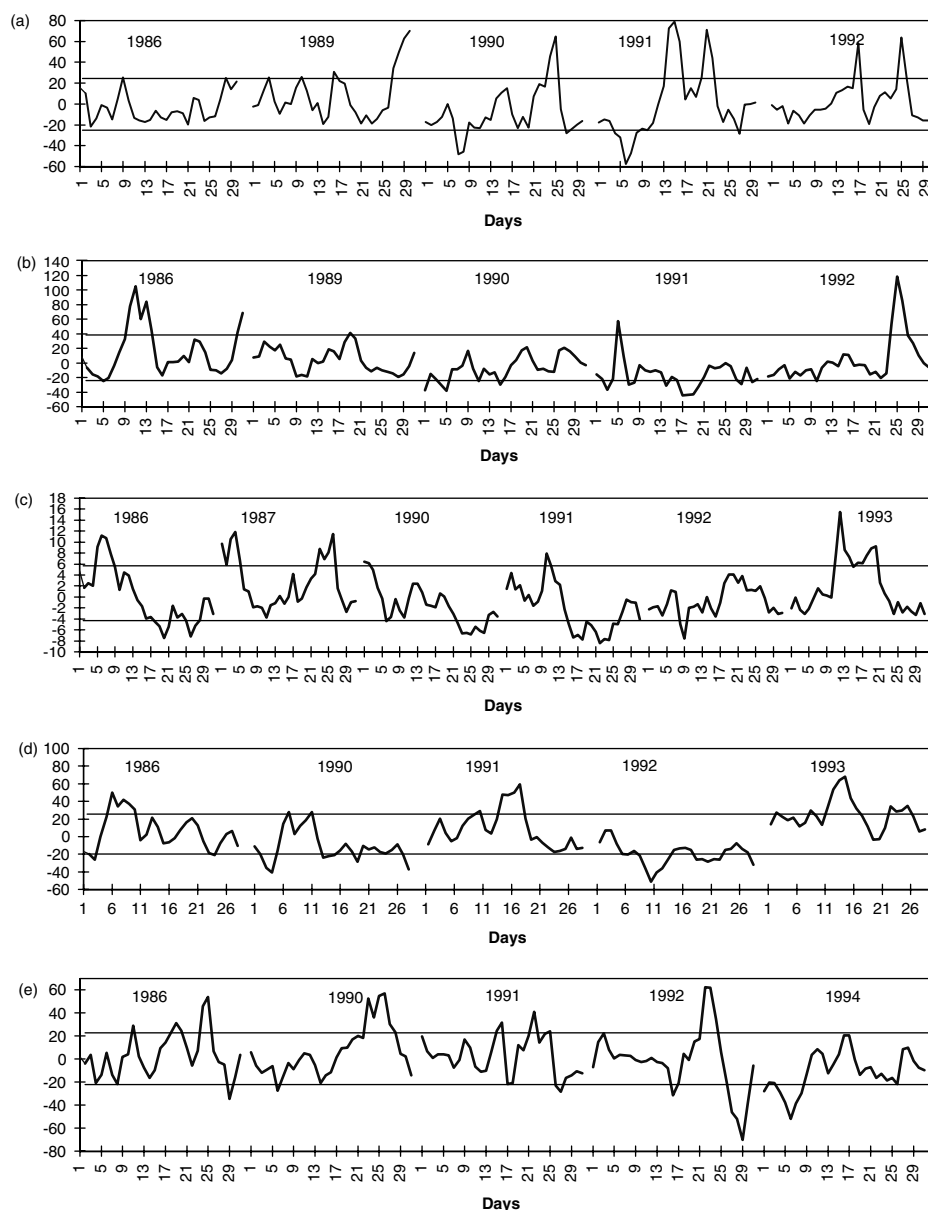


Figure 3. Time coefficients of EOF (with  $\pm 1$  standard deviation shown) for (a) November, (b) December, (c) January, (d) February, (e) March (adapted from Washington and Todd (1999))

### 3. RESULTS

#### 3.1. Mean structure of water vapour and transport during austral summer

During the austral summer months, the streamfunction component is larger than the divergent field (Figure 4(a) and (b)) such that total water vapour flux is well represented by the former (Chen, 1985). This rotational component of water vapour flux in the Southern Hemisphere is dominated by three centres of anticyclonic flow located over the subtropical latitudes of the Pacific, Atlantic and Indian Oceans (Figure 4(a)). The anticyclonic circulation over the Indian Ocean extends eastwards over continental subtropical SA. Mean atmospheric water vapour is concentrated in the tropics primarily in three regions: the equatorial west Pacific,

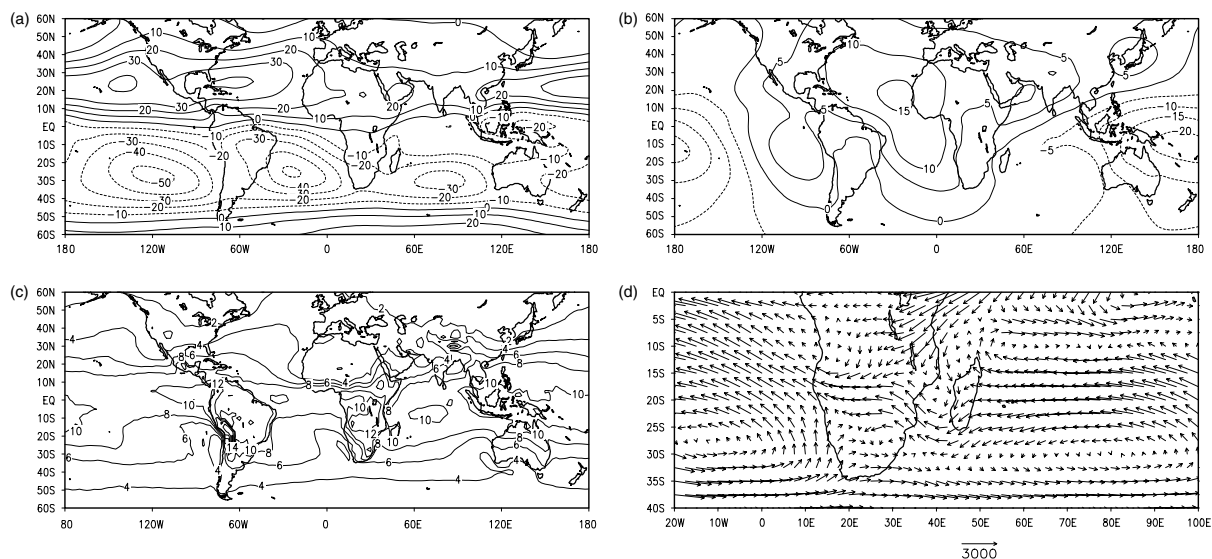


Figure 4. Mean December–February quantities: (a) non-divergent ( $\psi$ ) vertically integrated water vapour transport ( $10^8 \text{ kg s}^{-1}$ ), (b) divergent ( $\chi$ ) vertically integrated water vapour transport ( $10^8 \text{ kg s}^{-1}$ ), (c) 850 hPa specific humidity ( $\text{g kg}^{-1}$ ), and (d) vertically integrated vapour flux vectors ( $\text{kg m}^{-1} \text{ s}^{-1}$ )

northern South America and tropical southern Africa (Figure 4(c)). Chen (1985) demonstrated that this structure is maintained by the divergent stationary mode of water vapour flux, representing the Hadley and Walker circulations. The mean field of divergent water vapour flux in summer exhibits variations largely in the zonal dimension. Centres of convergence are broadly coincident with the three regions of high water vapour content identified above, strongly dominated by the west Pacific region (Figure 4(b)). Extensive regions of vapour divergence support this structure, with major centres over the tropical Atlantic Ocean and the tropical east Pacific Ocean. Thus, high values of mean water vapour over tropical SA are maintained by a divergent flux largely from the equatorial east Atlantic.

The mean vapour transport over SA and the SWIO (Figure 4(d)) indicates an easterly vapour flux into SA equatorward of  $30^\circ\text{S}$  from the Indian Ocean region. This converges with a weaker northerly flux over tropical SA centred on  $12^\circ\text{S}$ , which results from a weak cyclonic circulation centred over western SA near  $12^\circ\text{S}$ , associated with the ITCZ. As the austral summer progresses, this feature becomes more pronounced, resulting in a westerly vapour flux over tropical SA in February (not shown). The annual seasonal cycle (not shown) results in other subtle, but important, differences between austral summer months over SA–SWIO. Of particular relevance is the progressive eastward displacement from early to late summer of the south Indian Ocean subtropical high (IOH), which weakens the anticyclonic circulation over SA.

### 3.2. Water vapour circulation associated with TTT events

**3.2.1. Early summer.** The rainfall EOF structure in the early summer months of November and December is remarkably similar, differing only in the detail of the TTT location. These months are therefore discussed together, using November as an exemplar. During November TTT events, the cloud bands extend from eastern SA (near  $15^\circ\text{S}$ ,  $30^\circ\text{E}$ ) across Mozambique out to the SWIO to provide a band of positive rainfall anomalies oriented NW–SE (Figure 5(a)). This rain band is located under a lower level anomalous trough extending from the tropics into the midlatitudes (Figure 5(a)) associated with an anomalous ridge–trough–ridge structure across the region. This wave structure over SA–SWIO is baroclinic, such that the rain band lies at the leading edge of the trough at upper levels (not shown). A pronounced poleward water vapour flux occurs between  $0^\circ\text{N}$  and  $50^\circ\text{S}$  driven by three main paths of anomalous water vapour flux (Figure 5(a)), namely: (a) a northerly flux from the northern Indian Ocean linked to a coherent zonal easterly flux between  $120$  and  $45^\circ\text{E}$  centred on

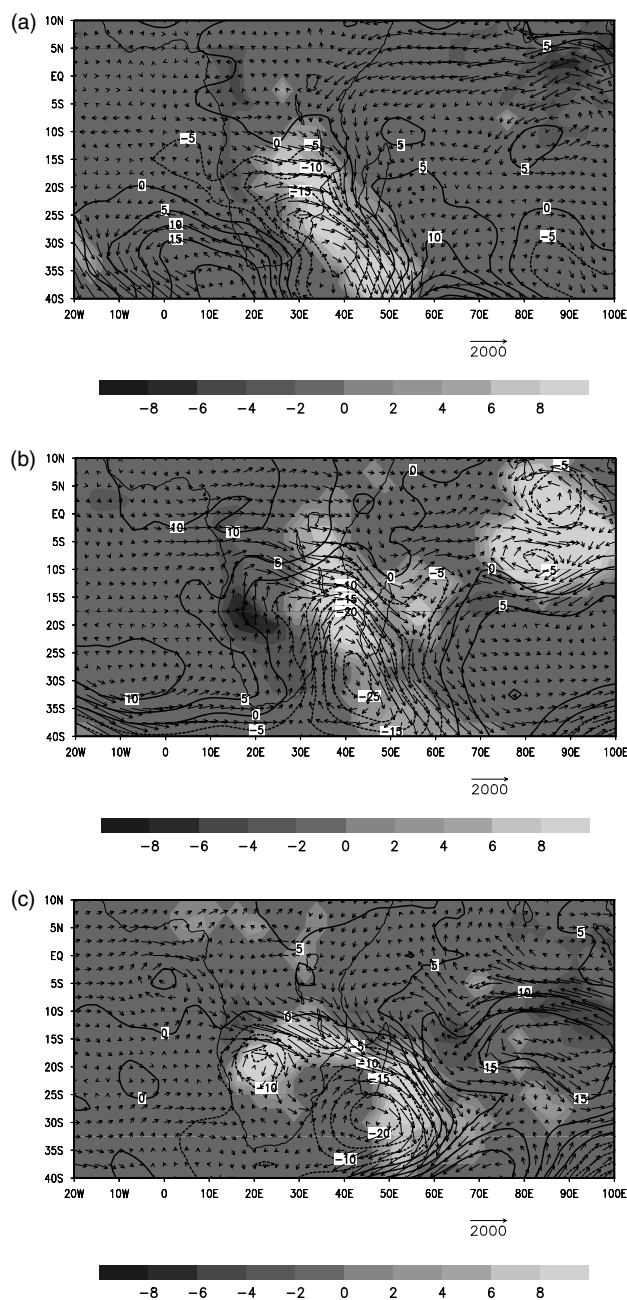


Figure 5. Composite anomaly fields of precipitation ( $\text{mm day}^{-1}$ , shaded), 850 hPa geopotential height (m, contours), and vapour flux anomalies ( $\text{kg m}^{-1} \text{s}^{-1}$ ) for (a) November positive TTT events, (b) January positive TTT events, and (c) February positive TTT events. Only those precipitation anomalies significant at the 0.05 level are displayed; all others are set to zero

5°N; (b) a westerly flux from western SA centred on 10°S; (c) a cyclonic flow around the TTT. Convergence of these three water vapour conduits occurs in the Mozambique Channel, near 20°S, and feeds into the TTT rain band.

The TTT axis is a zone of strong anomalous and absolute (not shown) water vapour convergence (Figure 6(a)) extending from eastern tropical SA near Lake Malawi extending along the TTT axis into the



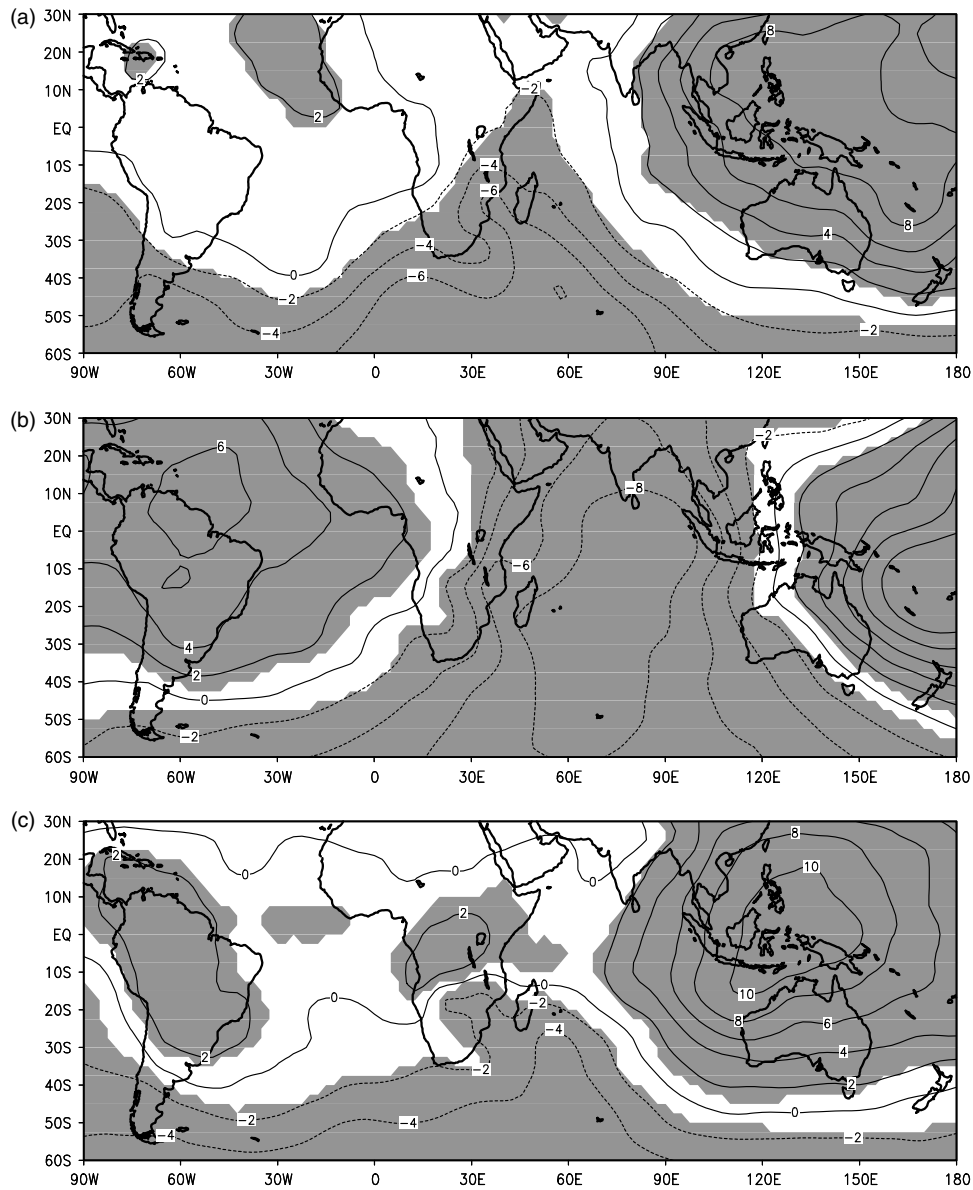


Figure 6. Composite mean anomalies of the divergent component  $\chi$  of vertically integrated water vapour transport ( $10^8 \text{ kg s}^{-1}$ ) for (a) November positive TTT events, (b) January positive TTT events, and (c) February positive TTT events. Contour units are  $2 \times 10^8 \text{ kg s}^{-1}$  and anomalies significant at the 0.05 level are shaded

midlatitude Southern Ocean near  $60^\circ\text{E}$ . This convergent flux is clearly associated with the deep convection and positive rainfall anomalies observed (Figure 5(a)). Notably, there are large positive  $\chi$  anomalies over the tropical west Pacific and maritime continent (centred on  $130^\circ\text{E}$ ,  $0^\circ\text{N}$ ), where the normally intense water vapour convergence is heavily suppressed. Anomalous divergence also occurs over the tropical Atlantic centred near  $15^\circ\text{N}$ ,  $15^\circ\text{W}$ , where the mean divergence is already strong. This anomalous divergence also extends over the region of vapour convergence over South America. Remarkably, most of the Southern Hemisphere poleward of  $40^\circ\text{S}$  experiences anomalous and absolute (not shown) vapour flux convergence.

The composite anomaly  $\psi$  field shows an enhanced anticyclonic circulation in the Indian Ocean centred on  $5^\circ\text{S}$ , extending poleward into the midlatitudes (Figure 7(a)). This occurs due to an intensification of the

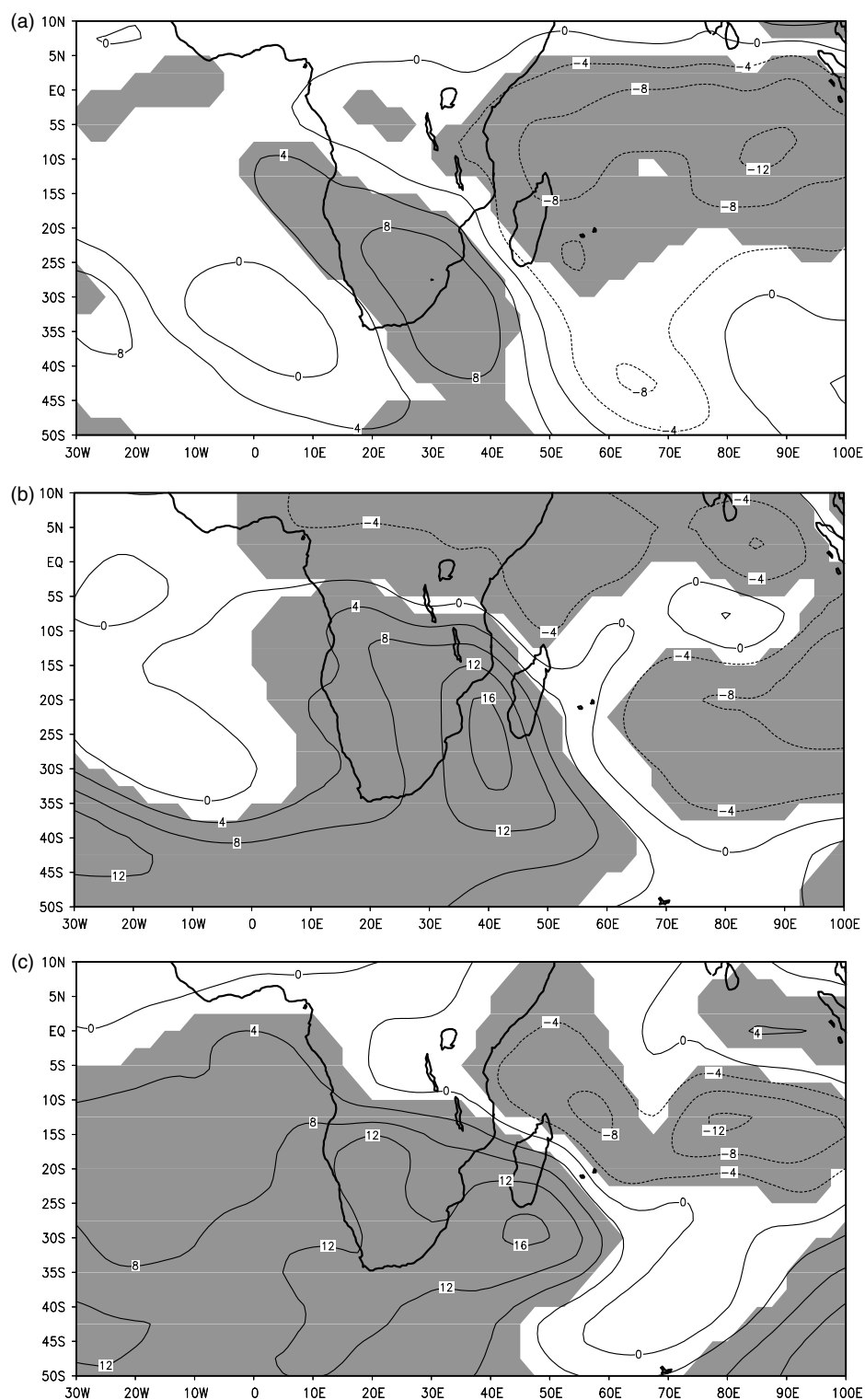
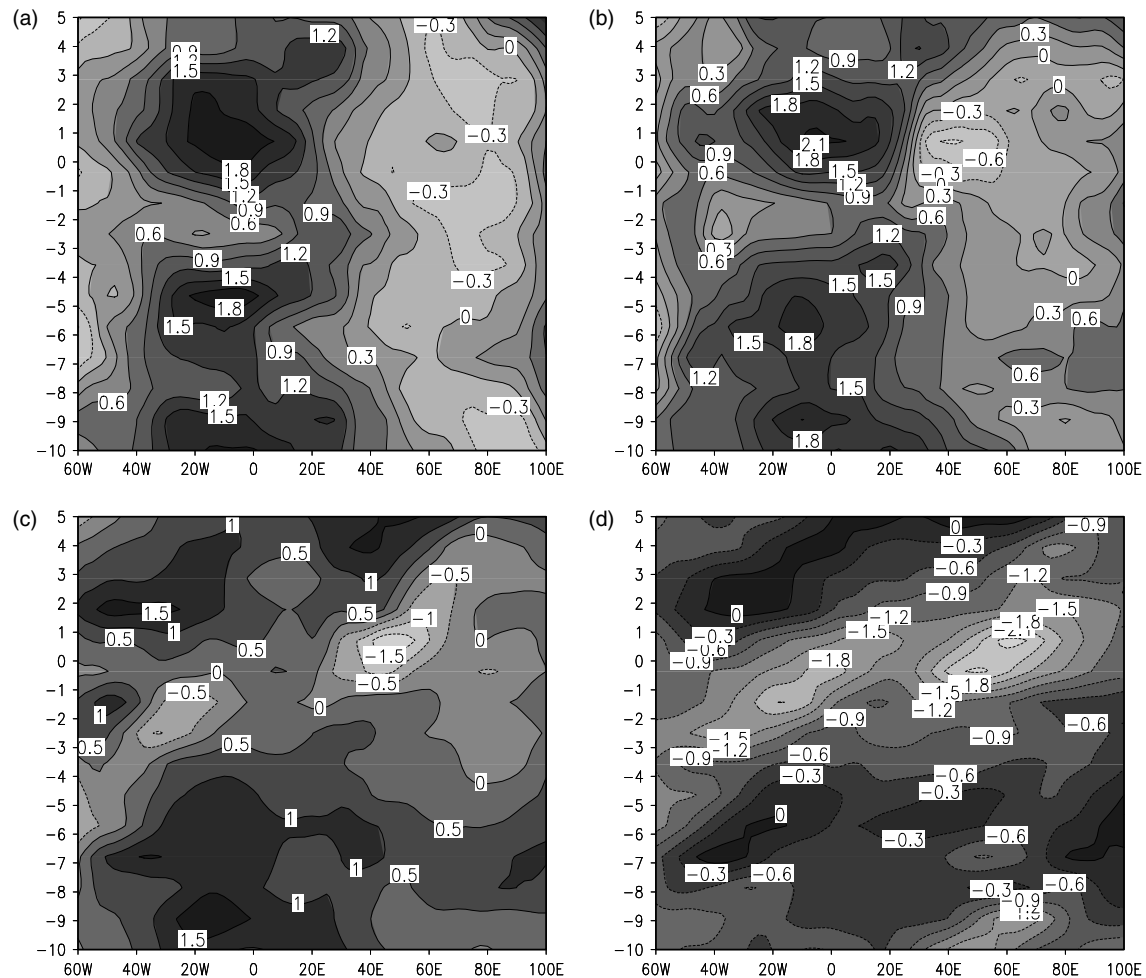


Figure 7. As Figure 6, except for the rotational (streamfunction) component  $\psi$  ( $10^8 \text{ kg s}^{-1}$ )

IOH, which is displaced northeastward from its mean position. The mean anticyclonic circulation weakens over eastern South Africa and the Mozambique Channel to the south such that a pronounced anomalous cyclonic flow associated with the TTT is apparent. Along the TTT axis composite mean streamfunction exceeds the divergent flux by almost an order of magnitude (not shown), but the anomalous fluxes are of a similar magnitude (Figures 6(a) and 7(a)).

Hovmoeller plots of  $\chi$  composites (Figure 8) show that water vapour divergent flux exhibits a pulsing at approximately 5-day intervals in the latitude bands centred on 10°N and 10°S. Within the band centred on 10°S a major intensification of divergence centred on 10°W and convergence on 40°E develops, beginning around 1 day prior to the TTT event. The eastward propagation of the convergent water vapour flux in the bands centred on 40°S and 50°S can be traced for up to 8 days prior to the TTT event, but a major intensification also occurs 1 day prior to the TTT event. A weakening of divergence over the source region in the eastern tropical Atlantic occurs in association with the dissipation of the TTT system.

**3.2.2. Late summer.** Both the daily rainfall EOF loading patterns and the structure of water vapour flux differ between January and February, such that these will be considered separately.



*3.2.2.1. January:* During January TTT events, positive rainfall anomalies extend NW–SE from the Great Lakes region of East Africa out to the SWIO (Figure 5(b)). As in early summer, this rain band is coincident with a low-level anomalous trough extending from the tropics into the midlatitudes (Figure 5(b)), associated with a baroclinic ridge–trough–ridge wave structure at upper levels (not shown). January water vapour flux anomaly composites (Figure 5(b)) are similar to those discussed for early summer, but with some important differences. First, there is a more southerly location of the anomalous easterly water vapour flux across the Indian Ocean (centred on 15°S rather than 5°N in November). Second, the anomalous westerly flux from western SA near 10°S is strengthened such that the flux is westerly in absolute terms (not shown). Consequently, convergence of moisture occurs near 10–20°S and 55°E, somewhat further east than in early summer (Figure 5(b)).

As in early summer, the TTT region is characterized as a zone of absolute vapour flux convergence (not shown) and convergent flux anomalies (Figure 6(b)), extending from eastern tropical SA near Lake Malawi to the SWIO along the TTT rain band. However, this occurs in conjunction with larger convergent anomalies in a broad zone across the tropical Indian Ocean to 120°E. These anomalies are coincident with positive rainfall anomalies over the eastern Indian Ocean (Figure 5(b)) not directly associated with TTT systems over SA–SWIO, such that the  $\chi$  anomaly field over the Indian Ocean does not reflect TTT systems as clearly as in other months. Anomalous vapour flux divergence is again observed over the tropical Atlantic and South American sector (centred near 10°N, 50°W) and also over the equatorial central Pacific region, centred on 15°S, 160°E. As in early summer, there is hemispheric-wide anomalous and absolute (not shown) convergence throughout the mid and high latitudes of the Southern Hemisphere. Hovmoeller plots (not shown) indicate a temporal variability in the intensity of divergence over the eastern tropical Atlantic region (centred on 10°N) similar to that during November positive events.

The  $\psi$  anomaly field (Figure 7(b)) is dominated by a large and pronounced cyclonic cell centred over the Mozambique Channel, extending NW over tropical east SA to west SA at 10°S (far to the north and west of that in early summer) and SE into the SWIO. The IOH is displaced westward and is intensified such that anomalous anticyclonic circulation occurs at 75°E. These circulation cells combine to produce a pronounced anomalous poleward transport of water vapour away from the zone of anomalous convergence in tropical east SA and the SWIO.

*3.2.2.2. February:* The TTT rain band links central and southeast SA (extending further west than in January) with the SWIO (Figure 5(c)). This is associated, characteristically, with negative low-level (and upper-level) geopotential height anomalies, with the TTT rain band over the SWIO located at the leading edge of the upper-level disturbance (not shown). Water vapour flux anomalies (Figure 5(c)) are similar to other months described here, except that the anomalous moisture flux into the TTT region emerges largely from only two regions, namely the Indian Ocean and tropical SA, centred on 12°S. The main convergence of moisture is east of Madagascar, near 60°E. The  $\chi$  field (Figure 6(c)) shows vapour convergence over the TTT region as in the other months studied. Divergent vapour flux anomalies (Figure 6(c)) are greatest over the maritime continent (similar to November), and a centre of weaker anomalous divergence occurs over the Congo basin centred on 25°E, 5°S. The rotational component of the water vapour circulation (Figure 7(c)) is similar to January positive events

#### 4. DISCUSSION

The results of this study provide new insights into relationships amongst the atmospheric circulation, water vapour flux and rainfall over SA and the SWIO region. The work is novel in terms of the nature of the data and sampling basis. Using daily satellite rainfall estimates over both land and ocean, together with the NCEP reanalysis data, we are able to resolve specific synoptic conditions (representing the dominant rainfall systems in the region) and the associated atmospheric circulation structure. This contrasts with numerous previous studies in which rainfall data over SA are used as the basis for sampling anomalously wet or dry conditions over the continent only.

Composite analysis reveals that TTT rain bands over SA–SWIO are zones of pronounced water vapour convergence extending from equatorial SA to the midlatitudes, in accordance with the suggestions of Harrison (1984, 1986). This vapour sink supports the deep convection and rainfall anomalies observed during TTTs. Previous work (Chen, 1985) indicates that the divergent component of the standing mode of water vapour transport maintains the high levels of precipitable water and rainfall observed over equatorial SA. This represents the regional Walker circulation. Our results suggest that TTT events are associated with an increase in the intensity of the African Walker cell, with enhanced water vapour convergence over tropical SA.

Water vapour converging over equatorial SA is transported poleward along the TTT cloud band through a coupling of cyclonic circulation to the west and by an anticyclonic circulation to the east of the TTT axis. Maximum poleward transport occurs along the leading easternmost edge of the temperate disturbance, as suggested by Harrison (1986). This circulation is largely represented by the vapour streamfunction. The anomalous streamfunction component flux consists of an anomalously strong IOH, displaced eastward from its mean position, and a cyclonic circulation located over the continent (where the midlatitude transient links with the continental low). That the cyclonic circulation over central continental SA is associated with a convergence of water vapour may indicate the importance of water vapour to the maintenance of this circulation.

As a proportion of the respective mean values, anomalies in the divergent flux are far greater than those of the streamfunction. Chen (1985) calculated that the poleward transport of vertically integrated water vapour is carried out essentially by the transient component of the circulation and that this is described largely by the divergent component with a maximum in the midlatitudes. The composites associated with TTT events also show a convergent flux into the mid and high latitudes, confirming the role of TTTs over SA in this process. Indeed, the reorganization of the divergent vapour flux field globally during these TTT events is remarkable. There are major adjustments to the Walker circulation globally, with anomalous divergence observed over the net vapour sink regions of the west and central Pacific Oceans and South America, and a pronounced vapour convergence throughout the high latitudes of the Southern Hemisphere.

Comparison of the individual summer months highlights important seasonality in the nature of TTT events and the associated water vapour transport fields. TTT events during late summer months tend to have a preferential location over the SWIO associated with the eastward progression of the IOH over the summer season, and increased thermal forcing of an upper-level westerly wave over SA, whose leading edge lies over Madagascar in high summer (Harrison, 1986). Development of a continental low over western tropical SA in late summer enhances the low level westerly flow from western SA at 10°S, facilitating anomalous water vapour convergence over eastern SA. This links with the TTT cloud band, such that the resulting feature extends further west over SA than in early summer. During February, water vapour convergence is supported by anomalous divergence over western SA. Therefore, in agreement with D'Abreton and Tyson (1995) we can infer that the role of tropical circulation in controlling water vapour transport in late summer is greater than in early summer when the midlatitude circulation dominates. The results support the conclusion of D'Abreton and Tyson (1995), that TTT cloud bands emerge from a coincidence of tropical and midlatitude disturbances and depend upon specific fields of water vapour divergence (convergence) over the tropical oceans (Africa) to maintain the necessary moisture into the system.

This study uncovers only limited evidence of divergence over the Indian Ocean north of Madagascar as a key source region in maintaining water vapour in tropical Africa, as identified by D'Abreton and Tyson (1995) during both wet early and late summers over SA. The dominant feature in all TTT events is anomalous divergence over the maritime continent/west Pacific combined with weaker anomalous divergence over the tropical SE Atlantic. This structure of water vapour transport during positive events is broadly in line with model simulations of the mean December SICZ feature (Cook, 2000). In addition, the results of D'Abreton and Tyson (1995) indicate that dry conditions over SA are associated with a northward non-divergent transport of converged water vapour, in contrast to the structure of positive events here. The differences between these findings and those of D'Abreton and Tyson (1995) are likely to result from the respective sampling used. Whereas this study resolves major TTT events explicitly, the D'Abreton and Tyson (1995) study considers wet and dry months over SA, to which TTTs make only a partial contribution.

## 5. SUMMARY AND CONCLUSIONS

It is now well established that TTT systems are the dominant rain-producing synoptic type over SA and the SWIO, and that they represent an important mechanism of poleward transport of energy, water vapour and momentum (Harrison, 1986; Todd and Washington, 1998; Washington and Todd, 1999; Palmer *et al.*, 2004). The significance of both tropical and extratropical dynamics in the development of TTT cloud bands has been demonstrated (Todd and Washington, 1999a). This paper provides further insight into the transport of water vapour in TTT systems during the austral summer months, derived from an objective sampling basis of land and oceanic rainfall. We calculate the rotational (streamfunction) and divergent components of vertically integrated water vapour transport. The total flux is largely accounted for by the streamfunction, but the divergent component is related to rainfall through the water balance equation.

The results indicate that major TTT events involve a pronounced poleward flux of water vapour along the rain band axis from the tropics deep into the midlatitudes. This transport is largely described by the streamfunction, which features an enhanced anticyclonic circulation to the east of the rain band (around a displaced IOH), combined with a cyclonic circulation to the west, extending from 10°S into the midlatitudes. TTT events emerge as large features of net water vapour convergence extending from equatorial SA to the midlatitudes. As such, the divergent circulation maintains the water vapour necessary for rainfall along the rain band.

Indeed, adjustments to the divergent component are relatively more important than those in the streamfunction. The enhanced water vapour convergence over tropical SA and the SWIO during TTT events is associated by adjustments to the Walker circulation, most notably involving anomalously weak convergence over the maritime continent and west Pacific. Moreover, vapour convergence occurs throughout the high latitudes of the Southern Hemisphere. It has been suggested that rainfall over SA is likely to be driven by one or both of the other three (larger) zones regions of Southern Hemisphere summer convection (Tyson, 1986). We show that TTT events are associated with enhanced divergence in the primary source region over the SE tropical Atlantic but that the greatest anomalies occur east of SA over the maritime continent and west Pacific, where convergence is heavily suppressed.

## ACKNOWLEDGEMENTS

We are grateful to the University of Oxford for support.

## REFERENCES

- Adams JC, Swartrauber PN. 1997. SPHEREPACK 2.0: a model development facility. NCAR Technical Note NCAR/TN-436-STR.
- Chen TC. 1985. Global water vapour flux and maintenance during FGGE. *Monthly Weather Review* **113**: 1801–1819.
- Cohen AL, Tyson PD. 1995. Sea-surface temperature fluctuations during the Holocene off the south coast of Africa: implications for terrestrial climate and rainfall. *The Holocene* **5**: 304–312.
- Cook KH. 2000. The south Indian convergence zone and interannual rainfall variability over southern Africa. *Journal of Climate* **13**: 3789–3804.
- Cook KH. 2001. A Southern Hemisphere wave response to ENSO with implications for southern Africa precipitation. *Journal of the Atmospheric Sciences* **58**: 2146–2162.
- D'Abreton PC, Lindsay JA. 1993. Water vapour transport over southern Africa during wet and dry early and late summer months. *International Journal of Climatology* **13**: 151–170.
- D'Abreton PC, Tyson PD. 1995. Divergent and non-divergent water vapour transport over southern Africa during wet and dry conditions. *Meteorology and Atmospheric Physics* **55**: 47–59.
- Diab RD, Preston-Whyte RA, Washington R. 1991. Distribution of rainfall by synoptic type over Natal. *South African Geographical Journal* **66**: 46–47.
- Folland CK, Parker D, Colman A, Washington R. 1998. Low frequency variability of worldwide ocean surface temperature in the historical record. In *Beyond El Niño: Decadal Variability in the Climate System*, Navarra A. (ed.). Springer-Verlag: Berlin; 73–102.
- Goddard L, Graham NE. 1999. Importance of the Indian Ocean for simulating rainfall anomalies over eastern and southern Africa. *Journal of Geophysical Research* **104**: 19 099–19 116.
- Harrison MSJ. 1984. A generalized classification of South African summer rain-bearing synoptic systems. *International Journal of Climatology* **4**: 547–560.
- Harrison MSJ. 1986. A synoptic climatology of South African rainfall variations. PhD thesis, University of Witwatersrand, South Africa.
- Janowiak J. 1988. An investigation of interannual rainfall variability in Africa. *Journal of Climate* **1**: 240–255.
- Jury MR. 1992. A climatic dipole governing the interannual variability of convection over the SW Indian Ocean and SE Africa region. *Trends in Geophysical Research* **1**: 165–172.

- Jury MR. 1997. Inter-annual climate modes over southern Africa from satellite cloud OLR 1975–1994. *Theoretical and Applied Climatology* **57**: 155–163.
- Jury MR, Pathack BMR, Sohn BJ. 1992. Spatial structure and interannual variability of summer convection over southern Africa and the SW Indian Ocean. *South African Journal of Science* **88**: 275–280.
- Kalnay E, Kanamitsu M, Kistler R, Collins W, Deaven D, Gandin L, Iredell M, Saha S, White G, Woollen J, Zhu Y, Leetmaa A, Reynolds R, Chelliah M, Ebisuzaki W, Higgins W, Janowiak J, Mo KC, Ropelewski C, Wang CJ, Jenne R, Joseph D. 1996. The NCEP/NCAR 40-year reanalysis project. *Bulletin of the American Meteorological Society* **77**: 437–471.
- Landman WA, Mason SJ. 1999. Change in the association between Indian Ocean sea surface temperatures and summer rainfall over South Africa and Namibia. *International Journal of Climatology* **19**: 1477–1492.
- Mason SJ, Jury MR. 1997. Climatic change and inter-annual variability over southern Africa: a reflection on underlying processes. *Progress in Physical Geography* **21**: 24–50.
- Nassor A, Jury MR. 1997. Intra-seasonal climate variability of Madagascar. Part 2: evolution of flood events. *Meteorology and Atmospheric Physics* **64**: 243–254.
- Nicholson SE, Kim J. 1997. The relationship of the El Niño–southern oscillation to African rainfall. *International Journal of Climatology* **17**: 117–136.
- Nicholson SE, Selato JS. 2000. The influence of La Niña on African rainfall. *International Journal of Climatology* **20**: 1761–1776.
- Nicholson SE, Leposo D, Grist J. 2001. The relationship between El Niño and drought over Botswana. *Journal of Climate* **14**: 323–335.
- Palmer PI, Heifetz E, Todd MC, Washington R. 2004. The meridional flux of angular momentum during major tropical–temperate rainfall events over southern Africa. *Climate Dynamics* submitted for publication.
- Parker BA, Jury MR. 1999. Synoptic environment of composite tropical cyclones in the south-west Indian Ocean. *South African Journal of Marine Science* **21**: 99–115.
- Piexoto JP, Oort AH. 1991. *Physics of Climate*. Springer-Verlag: New York.
- Rocha A, Simmonds I. 1997. Interannual variability of southeastern African summer rainfall, part 1: relationships with air–sea interaction. *International Journal of Climatology* **17**: 235–266.
- Stokes SD, Thomas SG, Washington R. 1997. Multiple episodes of aridity in southern Africa since the last inter-glacial. *Nature* **38**: 154–158.
- Streten NA. 1973. Some characteristics of satellite-observed bands of persistent cloudiness over the Southern Hemisphere. *Monthly Weather Review* **101**: 486–495.
- Todd MC, Washington R. 1998. Extreme daily rainfall in southern African and southwest Indian Ocean tropical–temperate links. *South African Journal of Science* **94**: 64–70.
- Todd MC, Washington R. 1999a. Circulation anomalies associated with tropical–temperate troughs over southern Africa and the southwest Indian Ocean. *Climate Dynamics* **15**: 937–951.
- Todd MC, Washington R. 1999b. A simple method to retrieve 3-hourly global tropical and subtropical rainfall estimates from ISCCP D1 data. *Journal of Atmospheric and Oceanic Technology* **16**: 146–155.
- Tyson PD. 1986. *Climatic change and variability in Southern Africa*. Oxford University Press: Cape Town.
- Washington R, Todd MC. 1999. Tropical temperate links in southern African and southwest Indian Ocean daily rainfall. *International Journal of Climatology* **19**: 1601–1616.
- Xie P, Arkin PA. 1997. Global precipitation: a 17year monthly analysis based on gauge observations, satellite estimates and numerical model outputs. *Bulletin of the American Meteorological Society* **78**: 2539–2558.